Separation Science and Technology
Publication details, including instructions for authors and subscription information:
http://www.informaworld.com/smpp/title~content=t713708471

A Microhydrodynamic Model of the Sedimentation Process

M. Nonaka[a]; T. Uchio[a]
[a] DEPARTMENT OF MINERAL DEVELOPMENT ENGINEERING, THE UNIVERSITY OF TOKYO, TOKYO, JAPAN

To cite this Article Nonaka, M. and Uchio, T.(1984) 'A Microhydrodynamic Model of the Sedimentation Process', Separation Science and Technology, 19: 4, 337 — 355
To link to this Article: DOI: 10.1080/01496398408068587
URL: http://dx.doi.org/10.1080/01496398408068587

SEPARATION SCIENCE AND TECHNOLOGY, 19(4 & 5), pp. 337-355, 1984

A Microhydrodynamic Model of the Sedimentation Process

M. NONAKA and T. UCHIO

DEPARTMENT OF MINERAL DEVELOPMENT ENGINEERING
THE UNIVERSITY OF TOKYO
TOKYO 113, JAPAN

Abstract

A microhydrodynamic model is proposed to evaluate the turbulent transport effects on the sedimentation behavior of fine solid particles. The model is deduced from a material balance in a turbulent field which includes concentration effects on the turbulent diffusion coefficients and the settling velocities of solid particles. The microhydrodynamic model can simulate the practical sedimentation behavior of solid particles not only in the steady state but also in the dynamic as well as the decay state.

INTRODUCTION

Processing of fine or ultrafine particles has been essential for separation operations involved not only in particulate processes but also in water treatment processes in which sedimentation of solid particles in gravity or a centrifugal field plays an important part. Most practical sedimentation processes must operate in turbulent states. Fine solid particles have only limited inertia and, hence, their sedimentation behavior is strongly affected by turbulent motion in the surrounding fluid.

Turbulent transport phenomena have been determined to be essential factors affecting the separation efficiencies in some separation processes (*1*–*8*). Thus it has been considered that homogeneous turbulent diffusion dominates separation processes. In sedimentation processes, however, turbulent energy supplied from a localized source will not be propagated homogeneously into the suspension because of the segregated solids

 0149-6395/84/1904-0337$3.50/0

concentration. Hence, the effect of turbulence on the sedimentation behavior of solid particles has to be described by a transport equation taking into consideration the dependence on the solid concentration.

The authors started with a theoretical consideration on the particle behavior in a turbulent field which could be evaluated by a material balance equation. Mass transfers due to turbulent diffusion and gravity settling were defined as functions of the solids concentration. Thus a microhydrodynamic model was proposed for the sedimentation process of fine particles. The experimental work was carried out by using the electrode reaction technique in order to observe the dependence of sedimentation behavior on turbulent characteristics and to verify the proposed model. Thus the exponential profile of the solids concentration conventionally accepted in the description of the vertical distribution of solids particles in a homogeneous turbulent field (*9*) has been revised through microhydrodynamic concepts.

MICROHYDRODYNAMIC MODEL

Consider material flows into and out of a minute space in a turbulent field involved in a continuous sedimentation process operated in a gravity field as shown in Fig. 1. The y coordinate is horizontal and at a right angle to the direction of flow in a rectangular clarifier; no variations are expected in this direction, so assuming $\delta y = 1$ is reasonable. Thus the material accumulation in the space per unit time due to the horizontal mean flow is described by

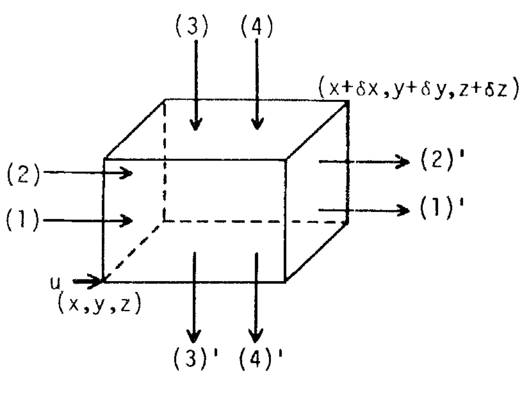

FIG. 1. Material flows in the sedimentation process. (1), (1)': due to main flow. (2), (2)': due to horizontal diffusion. (3), (3)': due to gravity settling. (4), (4)': due to vertical diffusion.

$$-\frac{\partial(u \cdot C_i)}{\partial x}\,\partial x\,\partial z$$

where u is the mean velocity of the horizontal flow and C_i is the concentration of solid particles in the ith class of size fractions on a volume basis.

The material accumulated due to gravity settling is

$$\frac{\partial(v_{s,i} \cdot C_i)}{\partial z}\,\partial x\,\partial z$$

where $v_{s,i}$ is the settling velocity of particles in the ith size fraction, while the material accumulation due to turbulent diffusion is

$$\frac{\partial}{\partial x}\left(D_{t,x}\frac{\partial C_i}{\partial x}\right)\partial x\,\partial z + \frac{\partial}{\partial z}\left(D_{t,z}\frac{\partial C_i}{\partial z}\right)\partial x\,\partial z$$

where the turbulent diffusion coefficients in the horizontal and vertical directions are assumed to be independent of the particle size. The solid concentration at a fixed point must not be changed in the steady state. Hence, in this state, the material balance is written as

$$\frac{\partial(u \cdot C_i)}{\partial x} = \frac{\partial(v_{s,i} \cdot C_i)}{\partial z} + \frac{\partial}{\partial x}\left(D_{t,x}\frac{\partial C_i}{\partial x}\right) + \frac{\partial}{\partial z}\left(D_{t,z}\frac{\partial C_i}{\partial z}\right) \tag{1}$$

The settling velocity and the turbulent diffusion coefficients should depend on the solids concentration. Assume here that they can be written as

$$v_{s,i} = v_{0,i}(1 - \alpha_1 \Sigma C_i)^{\alpha_2} \tag{2}$$

$$D_{t,x} = D_{0,x}(1 - \beta_1 \Sigma C_i)^{\beta_2} \tag{3}$$

$$D_{t,z} = D_{0,z}(1 - \beta_1 \Sigma C_i)^{\beta_2} \tag{4}$$

where $v_{0,i}$ is the settling velocity of a single particle in the ith size fraction, while $D_{0,x}$ and $D_{0,z}$ are the turbulent diffusion coefficients of a single particle in the x- and z-directions, respectively. The parameters α_1, α_2, β_1, and β_2 are determined by the physical properties, or especially rheological characteristics, of the solid–liquid system.

Then assuming that the horizontal mean velocity is uniformly distributed in the z-direction and also that the horizontal turbulent transportation can be disregarded, the sedimentation behavior observed in the coordinate system translating with the horizontal flow might be described by

$$\frac{d}{dz}\left(v_{s,i}\cdot C_i + D_{t,z}\frac{dC_i}{dz}\right) = 0 \tag{5}$$

Moreover, we can rewrite Eq. (1) as

$$\frac{\partial C_i}{\partial t} = \frac{\partial(v_{s,i}\cdot C_i)}{\partial z} + \frac{\partial}{\partial z}\left(D_{t,z}\frac{\partial C_i}{\partial z}\right) \tag{6}$$

which represents a batch sedimentation process. Then, putting $\alpha_2 = 0$ and $\beta_2 = 0$, the batch sedimentation behavior of solid particles can be revealed analytically in the steady state. It is given by

$$\frac{C_i}{C_{i,0}} = \exp\left\{-\frac{v_{s,i}}{D_{t,z}}(z - z_0)\right\} \tag{7}$$

where $C_{i,0}$ is the solids concentration on the level of $z = z_0$. Equation (7) has been widely accepted as the description of stationary batch sedimentation behavior in a homogeneous turbulent field (*9*). It should, however, be reasonable that Eq. (7) has to be revised by considering concentration effects on the settling velocity and the turbulent diffusion coefficient.

Homogeneous turbulence is rarely observed in practical sedimentation processes because locally supplied turbulent energy decays into the bulk of the suspension during propagation. Assuming that the energy spectrum function of turbulence is holomorphic at time $t = 0$ and is given by the first term of the Taylor expansion (*10*), the stochastic mean of the fluctuating velocities and the Eulerian integral space scale written as a decay process are given by

$$(\overline{u'^2})^{1/2} = \left(\frac{\sqrt{\pi}}{4}\gamma\right)^{1/2}(2\nu t)^{-5/4} \tag{8}$$

and

$$\Lambda_f = (2\pi\nu t)^{1/2} \tag{9}$$

except in the vicinity of the source of turbulence where γ is a constant determined by the energy spectrum function and ν is the kinematic viscosity (*10, 17*).

A stochastic mean of the fluctuating velocities observed at a short distance from the source of turbulence is denoted by $\sqrt{\overline{u_m'^2}}$. Then Eqs. (8) and (9) are rewritten as

$$(\overline{u'^2})^{1/2} = \left(\frac{\sqrt{\pi}}{4}\gamma\right)^{1/2}(2\nu)^{-5/4}\left\{t_0^{-1/4} - \frac{L}{2(\sqrt{\pi}\gamma)^{1/2}}(2\nu)^{5/4}\right\}^5 \quad (10)$$

and

$$\Lambda_f = (2\pi\nu)^{1/2}\left\{t_0^{-1/4} - \frac{L}{2(\sqrt{\pi}\gamma)^{1/2}}(2\nu)^{5/4}\right\}^{-2} \quad (11)$$

where t_0 is derived from

$$(\overline{u_m'^2})^{1/2} = \left(\frac{\sqrt{\pi}}{4}\gamma\right)^{1/2}(2\nu t_0)^{-5/4} \quad (12)$$

and L is the distance from the observed point. Hence, considering only vertical propagation of turbulent energy, the turbulent diffusion coefficient of the fluid element is given as a function of location by

$$D_{0,z} \equiv D_0 = \frac{\eta}{2}(\pi\sqrt{\pi}\gamma)^{1/2}(2\nu)^{-3/4}\left\{t_0^{-1/4} - \frac{L}{2(\sqrt{\pi}\gamma)^{1/2}}(2\nu)^{5/4}\right\}^3 \quad (13)$$

where η is the coefficient determined by the relation between Lagrangian and Eulerian turbulent characteristics, which has been recognized as 0.4 in homogeneous turbulence (*11*). Thus the sedimentation process described by Eq. (1) should be analyzed for by using Eqs. (4) and (13) in case locally supplied turbulent energy is propagated.

TURBULENT CHARACTERISTICS IN SEDIMENTATION PROCESS

Experimental

A number of methods, techniques, and instruments have been developed and used for the observation of the structure of turbulence, viz., hot wire or hot film anemometer methods, flow visualization techniques, electrochemical methods, utilization of pressure sensors, application of image analysis by photodiode arrays, utilization of laser Doppler effects, etc.

An electrode reaction method was selected for our experiment because turbulent characteristics could be detected on a minute scale and in a simple manner (*12*). Moreover, the electrode reaction technique can be applied to a system containing not only a continuous phase but also a dispersed phase. The reaction liquid consisted of potassium ferrocyanide, potassium ferricyanide, potassium chloride, and deionized water. The concentrations of these chemicals were 0.003, 0.003, and 0.2 mol/L, respectively. The reactions involved in this system are

$$Fe(CN)_6^{3-} + e \rightarrow Fe(CN)_6^{4-} \qquad \text{at cathode}$$

and

$$Fe(CN)_6^{4-} \rightarrow Fe(CN)_6^{3-} + e \qquad \text{at anode}$$

The diffusion current is determined by the flow velocity of the liquid in the vicinity of the cathode (*12, 13*).

The cathode was made of a platinum wire of 0.5 mm diameter which was sealed by glass except for the front surface, while a rectangular silver plate of 0.1 mm thickness was used as the anode. The experimental apparatus is shown in Fig. 2. A cylindrical tank made of transparent acrylic resin with an inner diameter of 240 mm was used as the sedimentation vessel for batch operation.

Solid particles were mixed with the reaction liquid to attain a predetermined level of the solid concentration in the sedimentation vessel. Then a fixed turbulent energy was supplied into the suspension through horizontally rotating rods which were arrayed at regular intervals in the vessel. The rods could also be partially detached in case turbulent energy was supplied heterogeneously into the suspension. The intensity of turbulence in the sedimentation vessel was controlled by the rotational speed of the horizontal rods.

The diffusion current between both electrodes was converted to voltage and then the analog signal was acquired at definite time intervals in the transient memory equipped with A/D converter. The digital output of the memory was transported to the microcomputer system in which turbulent characteristics were calculated.

The materials used were quartz and alumina particles. The former was distributed in sizes of less than 44 μm, while the latter was classified into fractions of five different sizes. The size distributions of the materials, as measured by a laser diffraction method (MICROTRAC), are illustrated in

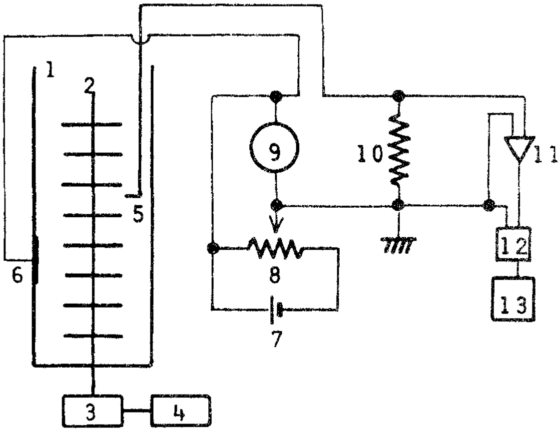

FIG. 2. Experimental system: (1) sedimentation vessel, (2) rotating rods, (3) motor, (4) controller, (5) cathode, (6) anode, (7) mercury battery, (8) rheostat, (9) volt meter, (10) standard resistance, (11) amplifier, (12) transient memory, (13) microcomputer system.

Fig. 3. Median will be accepted as a representative size of the classified alumina particles in the following description. The sedimentation behavior was observed by sampling through the pores arrayed on the side walls of the sedimentation vessel.

RESULTS AND DISCUSSION

It has been confirmed that the relation between the flow velocity of the suspension and the diffusion current is described by

$$I = a\sqrt{u} + b \tag{14}$$

where I is the diffusion current and u is the flow velocity, while a and b are constants determined by the properties of the electrodes and the solid–liquid system. The diffusion current as well as the flow velocity are composed of the mean and the fluctuating components. Hence, we can distinguish the fluctuating velocity by

$$u' = (I'/a)\{(I'/a) + 2\sqrt{\bar{u}}\} \tag{15}$$

where u' and I' denote the fluctuating components, while $\bar{u}$ is the mean velocity.

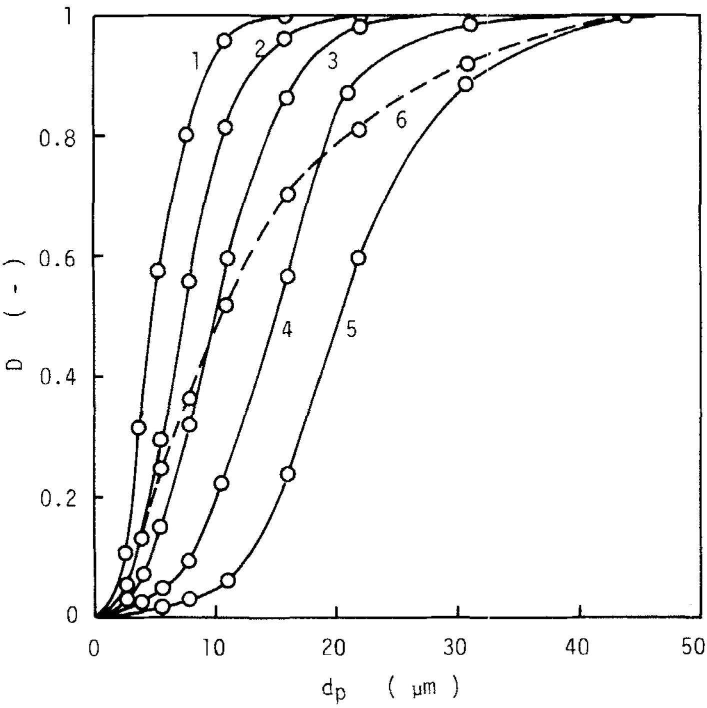

FIG. 3. Size distribution of materials: (1) alumina, $d_p = 5$ μm; (2) alumina, $d_p = 7.5$ μm; (3) alumina, $d_p = 10$ μm; (4) alumina, $d_p = 15$ μm; (5) alumina $d_p = 20$ μm; (6) quartz.

Dependence of the fluctuating velocity on the solids concentration was observed in relatively strong turbulent fields in which segregation of solid particles due to gravity settling was not completely realized. The results in the case of alumina particles are shown in Fig. 4, where u_0' denotes the fluctuating velocity of the medium containing only the continuous phase and all data have been observed in the case where constant turbulent energy was supplied into a unit mass of the suspension per unit time. Thus we can predict the relation between the fluctuating velocity and the solid concentration as

$$(\overline{u'^2})^{1/2} = (\overline{u_0'^2})^{1/2}(1 - \xi_1 \Sigma C_i)^{\xi_2} \tag{16}$$

where ξ_1 and ξ_2 are constants determined by the physical properties of the suspension and u'_0 can also be considered as the fluctuating velocity of a fine single particle. Moreover, Eq. (16) has been confirmed to be valid for a suspension containing quartz particles in a polydispersed state.

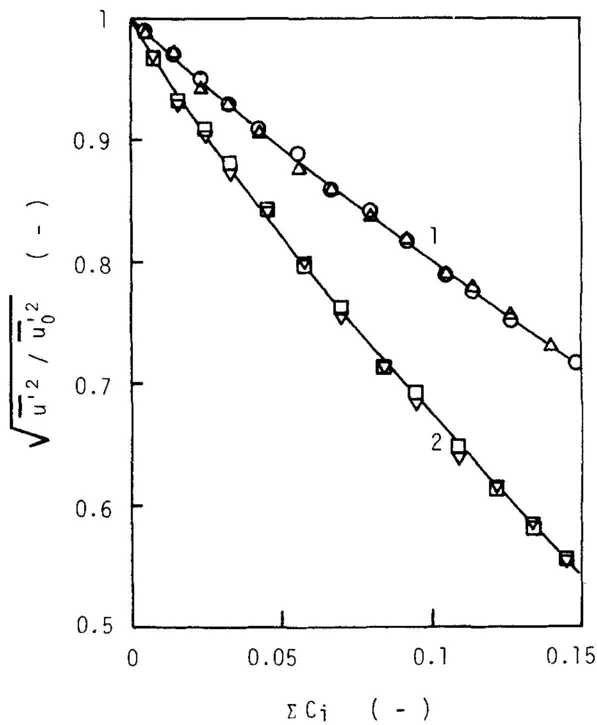

FIG. 4. Dependence of the fluctuating velocity on the solid concentration: (1) alumina, $d_p = 20$ μm, (○) $D_0 = 1.13 \times 10^{-5}$ m²/s, (△) $D_0 = 1.82 \times 10^{-5}$ m²/s; (2) alumina, $d_p = 5$ μm, (□) $D_0 = 1.13 \times 10^{-5}$ m²/s, (▽) $D_0 = 1.82 \times 10^{-5}$ m²/s.

Effects of the solid concentration on the time and space scale of turbulence have been discussed in terms of the Eulerian correlation function of the fluctuating velocities. The Eulerian velocity correlation function, defined by

$$R_E(\tau) = \overline{u'(t) \cdot u'(t+\tau)}/\overline{u'^2} \tag{17}$$

is shown in Fig. 5. Thus it is found that the correlation function can be written as

$$R_E(\tau) = \exp\left(-\frac{\pi\tau^2}{4T_E^2}\right) \tag{18}$$

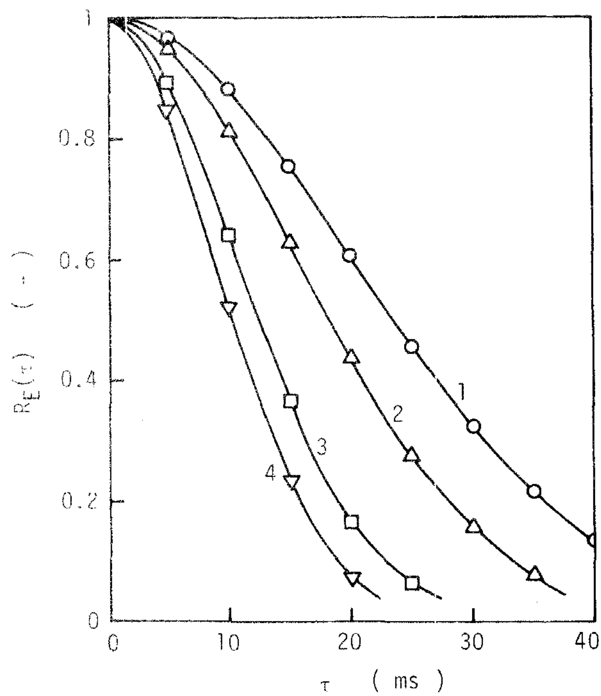

FIG. 5. Eulerian velocity correlation function at $\Sigma C_i = 0.15$: (1) quartz, $D_0 = 1.13 \times 10^{-5}$ m^2/s; (2) alumina ($d_p = 20$ μm), $D_0 = 1.13 \times 10^{-5}$ m^2/s; (3) quartz $D_0 = 1.82 \times 10^{-5}$ m^2/s; (4) alumina ($d_p = 20$ μm), $D_0 = 1.82 \times 10^{-5}$ m^2/s.

where T_E is the Eulerian integral time scale defined by

$$T_E = \int_0^\infty R_E(\tau)\, d\tau \tag{19}$$

The integral time scale should be affected by the physical properties of the suspension as shown in Fig. 5.

Another scale of turbulence, or the integral space scale, should be derived from the longitudinal or the transverse velocity correlation function. We can, however, define a space scale of turbulence more straightforwardly as

$$\Lambda_f = \bar{u} \cdot T_E \tag{20}$$

The space scale must be approximately consistent with the integral space scale of the longitudinal velocity correlation function. Therefore, the turbulent diffusion coefficient in the mean flow direction can be written as

$$D_t = \eta(\overline{u'^2})^{1/2} \cdot \Lambda_f \tag{21}$$

where η is equivalent to the coefficient involved in Eq. (13).

The effect of solid concentration on the turbulent diffusion coefficient in homogeneous turbulence is shown in Fig. 6, where solid lines are drawn through least square treatments according to the same functional form as Eqs. (3) and (4). As can be seen, the assumptions provided to build up the microhydrodynamic model must be reasonable. Moreover, Eq. (2), which represents the concentration effect on the settling velocity, has been widely used to analyze for the sedimentation behavior of solid particles (*3, 14–16*).

The propagation of turbulent energy locally supplied into the suspension has also been experimentally studied. The decay behavior of the fluctuating velocity in the case of a fixed turbulent energy supplied into a medium containing only a continuous phase in the vicinity of the surface level of the sedimentation vessel is illustrated in Fig. 7. In Fig. 7, the solid lines were drawn by using Eqs. (10) and (12). Thus it has been proved that these equations are validated for the description of the decay characteristics of turbulence, which has also been confirmed by the experimental verification of Eq. (11).

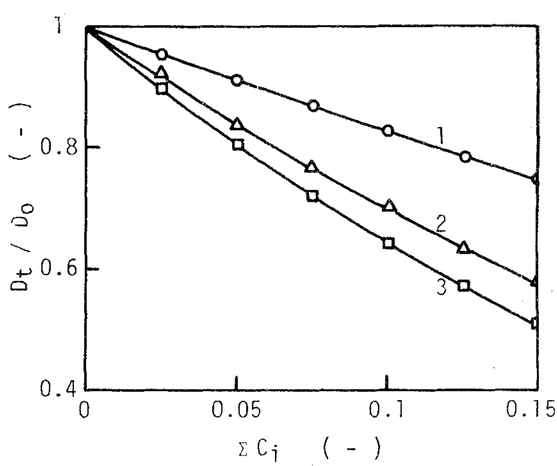

FIG. 6. Dependence of the turbulent diffusion coefficient on the solid concentration: (1) alumina, $d_p = 20$ μm; (2) alumina, $d_p = 5$ μm; (3) quartz.

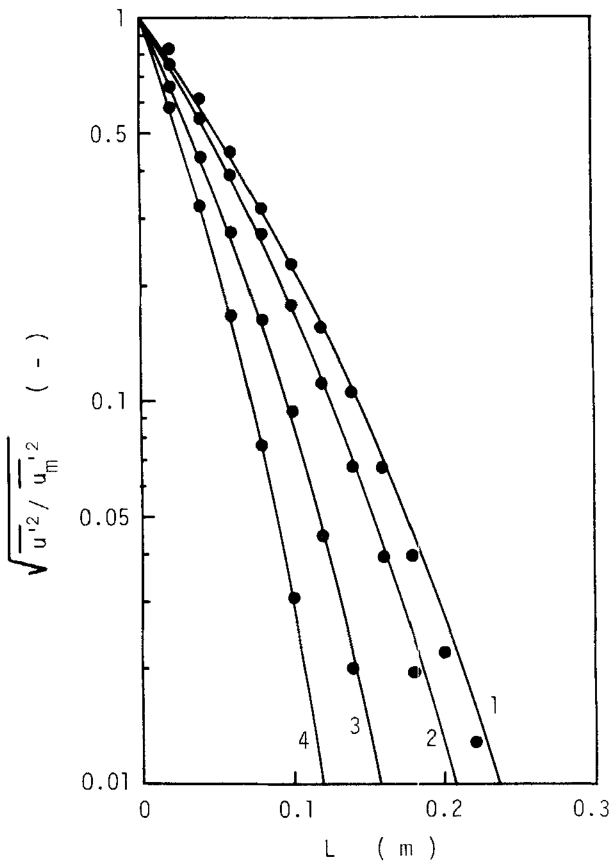

FIG. 7. Decay of the fluctuating velocity in continuous phase: (1) $D_0 = 1.22 \times 10^{-4}$ m²/s, (2) $D_0 = 8.04 \times 10^{-5}$ m²/s, (3) $D_0 = 3.64 \times 10^{-5}$ m²/s, (4) $D_0 = 2.40 \times 10^{-5}$ m²/s, (5) $D_0 = 1.58 \times 10^{-5}$ m²/s.

NUMERICAL ANALYSIS AND VERIFICATION

The proposed microhydrodynamic model has been evaluated from the viewpoint of solid concentration profiles in the sedimentation vessel. As a first step, the effects of the parameters involved in Eqs. (2) and (4) on the concentration profile have been numerically analyzed in various types of suspensions, some of which are shown in Fig. 8. The results were obtained by the batch sedimentation process in steady state where the sources of turbulent energy were uniformly distributed. Then a few of them were

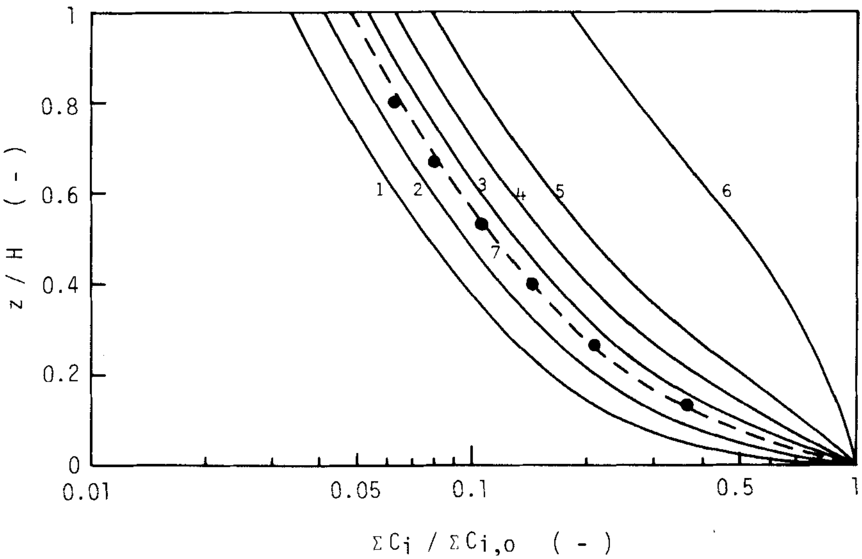

FIG. 8. Effects of the parameters α_1, α_2, β_1, and β_2 on the steady-state-concentration profile of polydispersed alumina particles ($d_p = 5$–20 μm) at $D_0 = 1.10 \times 10^{-5}$ m^2/s: (1) $\alpha_1 = 0$, $\alpha_2 = 0$, $\beta_1 = 2$, $\beta_2 = 4$; (2) $\alpha_1 = 0$, $\alpha_2 = 0$, $\beta_1 = 1$, $\beta_2 = 4$; (3) $\alpha_1 = 0$, $\alpha_2 = 0$, $\beta_1 = 0$, $\beta_2 = 0$; (4) $\alpha_1 = 0.5$, $\alpha_2 = 4$, $\beta_1 = 0$, $\beta_2 = 0$; (5) $\alpha_1 = 1$, $\alpha_2 = 4$, $\beta_1 = 0$, $\beta_2 = 0$; (6) $\alpha_1 = 2$, $\alpha_2 = 4$, $\beta_1 = 0$, $\beta_2 = 0$; (7) $\alpha_1 = 1$, $\alpha_2 = 3$, $\beta_1 = 1$, $\beta_2 = 4.5$. (Plots are experimental results.)

compared with experimental results observed in suspensions containing alumina particles.

We find that the larger the parameter β_1 or β_2, the more widely distributed is the concentration, while the parameter α_1 or α_2 has an inverse effect on the concentration profile. Moreover, it is confirmed that the practical sedimentation behavior can be explained by the microhydrodynamic concept, and that the conventional model, which has been derived by disregarding concentration effects on the turbulent diffusion coefficient as well as on the settling velocity, cannot draw a precise picture of the sedimentation behavior of solid particles in a turbulent field.

The dependence of sedimentation behavior on the intensity of turbulence has also been analyzed for and verified through a series of experiments carried out for various types of suspensions composed of classified alumina particles (Fig. 9). As can be seen, a small change in intensity has a significant effect on the concentration profile.

In order to evaluate the dynamic behavior of the sedimentation process, Eq. (6) has been numerically analyzed by the explicit finite difference

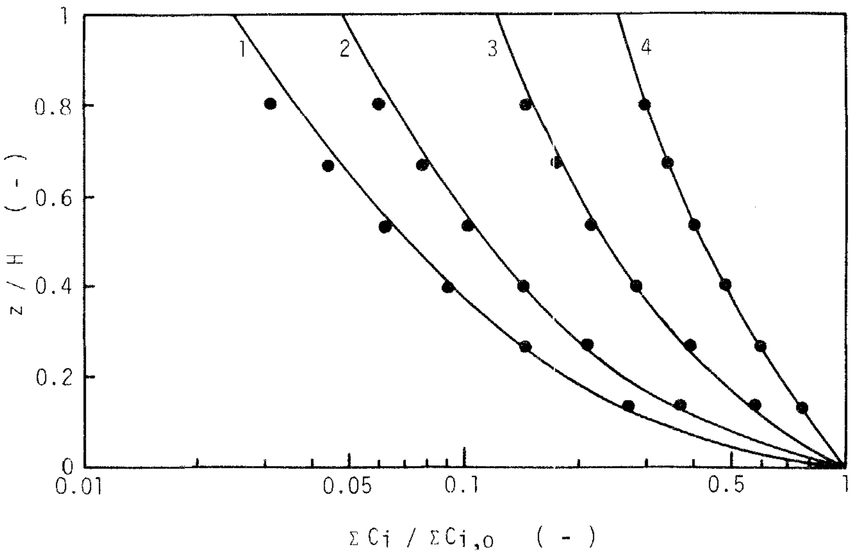

FIG. 9. Effect of the turbulent diffusion coefficient on the concentration profile of polydispersed alumina particles (d_p = 5–20 μm): (1) $D_0 = 7.50 \times 10^{-6}$ m²/s, (2) $D_0 = 1.10 \times 10^{-5}$ m²/s, (3) $D_0 = 2.20 \times 10^{-5}$ m²/s, (4) $D_0 = 4.60 \times 10^{-5}$ m²/s. (Solid lines correspond to $\alpha_1 = 1$, $\alpha_2 = 3$, $\beta_1 = 1$, and $\beta_2 = 4.5$, while plots are experimental results.)

method recently developed to solve nonlinear parabolic differential equations (*18*). Variations of the solid concentration on a fixed level with time are analyzed in turbulent fields where the sources of turbulence are uniformly located in the sedimentation vessel. Some of them are compared with experimental results and illustrated in Figs. 10 and 11. As can be seen, the solid concentration varies with time in a complicated manner through the intensity of turbulence and the particle size, especially in the initial stage of the process.

Turbulent energy is often locally supplied in the separation vessel in practical operation. In the sedimentation process this phenomenon can be observed in the case where the feed slurry is poured on the surface level of the sedimentation vessel or in the case where a disturbance is generated on the lower level of the vessel due to discharge of the sediments. Some of the numerical results obtained from Eqs. (2), (4), (6), and (13) in the steady state are shown in Figs. 12 and 13. In Fig. 12 the concentration profiles were obtained in a polydispersed system where the turbulent energy was supplied locally on the lower level of the suspension. The concentration profiles in a monodispersed system where turbulent energy was supplied on the upper level only are illustrated in Fig. 13. The numerical results are compared with

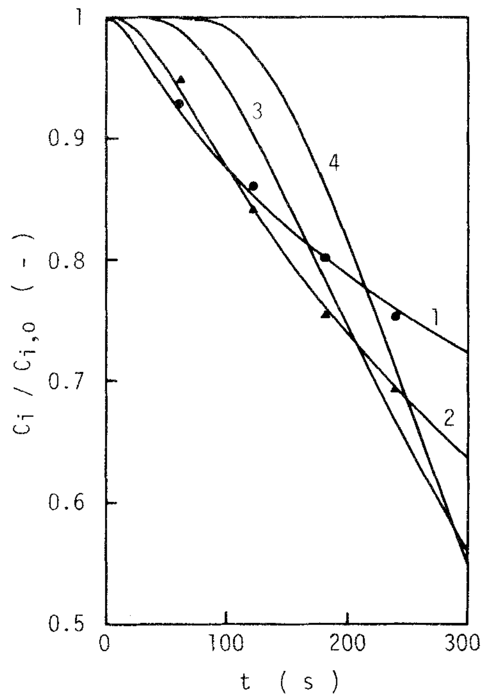

FIG. 10. Dynamic behavior of the sedimentation of monodispersed alumina particles (d_p = 10 μm) observed at $z/H = 0.87$: (1) $D_0 = 0.32 \times 10^{-4}$ m^2/s, (2) $D_0 = 0.11 \times 10^{-4}$ m^2/s, (3) $D_0 = 0.25 \times 10^{-5}$ m^2/s, (4) $D_0 = 0.10 \times 10^{-5}$ m^2/s. (Solid lines correspond to $\alpha_1 = 0.8$, $\alpha_2 = 3$, $\beta_1 = 0.8$, and $\beta_2 = 4.5$, while plots are experimental results.)

practical sedimentation behavior. They show satisfactory agreement under various conditions.

Thus it has been shown that the microhydrodynamic model deduced from a consideration of the dependence of the turbulent transport phenomena on the solid concentration can be more valid for a description of sedimentation behavior than the conventional model. It might, however, be somewhat more complicated to determine the parameters, depending on the physical properties of the suspension. The dependence on rheological properties of suspensions will be elucidated in future work.

CONCLUSIONS

A microhydrodynamic model has been derived from a simple mass balance equation in which mass transfers due to turbulent diffusion and

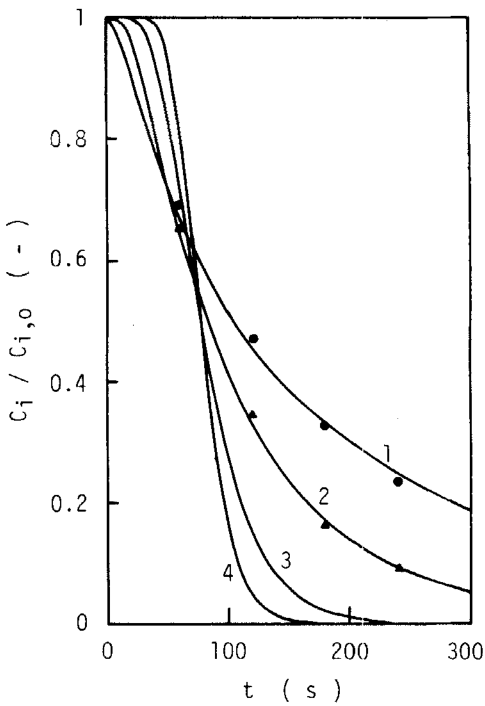

FIG. 11. Dynamic behavior of the sedimentation of monodispersed alumina particles ($d_p = 20\ \mu m$) observed at $z/H = 0.87$: (1) $D_0 = 0.32 \times 10^{-4}\ m^2/s$, (2) $D_0 = 0.11 \times 10^{-4}\ m^2/s$, (3) $D_0 = 0.25 \times 10^{-5}\ m^2/s$, (4) $D_0 = 0.10 \times 10^{-5}\ m^2/s$. (Solid lines correspond to $\alpha_1 = 0.65$, $\alpha_2 = 3$, $\beta_1 = 0.65$, and $\beta_2 = 4.5$, while plots are experimental results.)

gravity settling are considered to depend on the solids concentration. The dependence of the turbulent diffusion coefficient on the solids concentration in the sedimentation process has been verified through a series of experiments on the fluctuating velocity and the Eulerian velocity correlation function in a sedimentation vessel with a mixing device. The sedimentation process in heterogeneous turbulence has been analyzed by applying the decay theory of turbulence. The concentration profiles have been numerically analyzed for not only in the steady state but also in the dynamic state. They have been compared with practical sedimentation behavior and show good agreement. Thus the microhydrodynamic model has been shown to be a valid description of the sedimentation process progressing in a turbulent field.

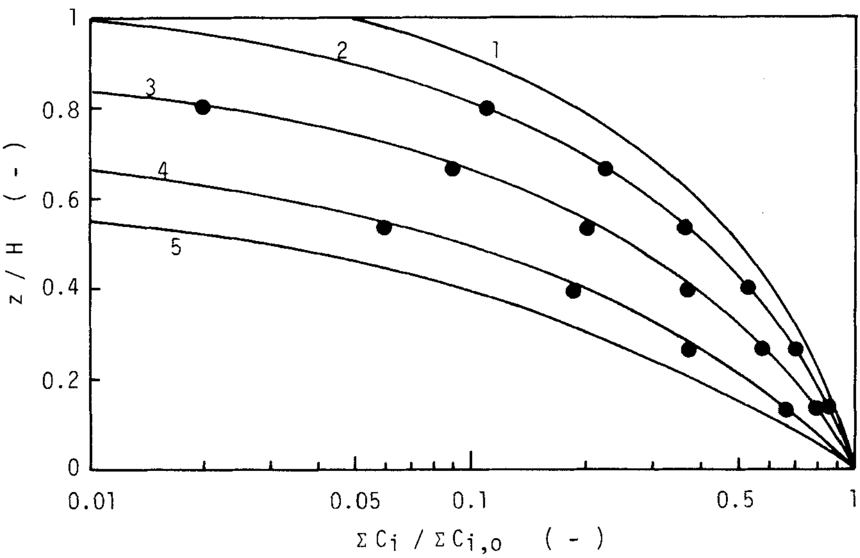

FIG. 12. Effect of the decay of turbulent energy supplied on the lower level of the suspension on the sedimentation behavior of polydispersed alumina particles ($d_p = 5$–20 μm): (1) $D_0 = 1.22 \times 10^{-4}$ m^2/s, (2) $D_0 = 0.95 \times 10^{-4}$ m^2/s, (3) $D_0 = 0.63 \times 10^{-4}$ m^2/s, (4) $D_0 = 0.36 \times 10^{-4}$ m^2/s, (5) $D_0 = 0.24 \times 10^{-4}$ m^2/s. (Solid lines correspond to $\alpha_1 = 1$, $\alpha_2 = 3$, $\beta_1 = 1$, and $\beta_2 = 4.5$, while plots are experimental results.)

Acknowledgments

The authors wish to thank Dr M. Honda of Showadenko Corp. Ltd. for the preparation of the materials and Mr S. Hamada in the graduate course of The University of Tokyo for a valuable contribution toward performing the numerical analysis. This work was supported partially by a Grant-in-Aid for Scientific Research No. 58550420 (1983) from the Ministry of Education, Science and Culture of Japan.

SYMBOLS

a, b	constants involved in Eq. (14)
C_i	concentration of solid particles in ith class of size fraction (—)
$C_{i,0}$	C_i at $z = z_0$ (—)

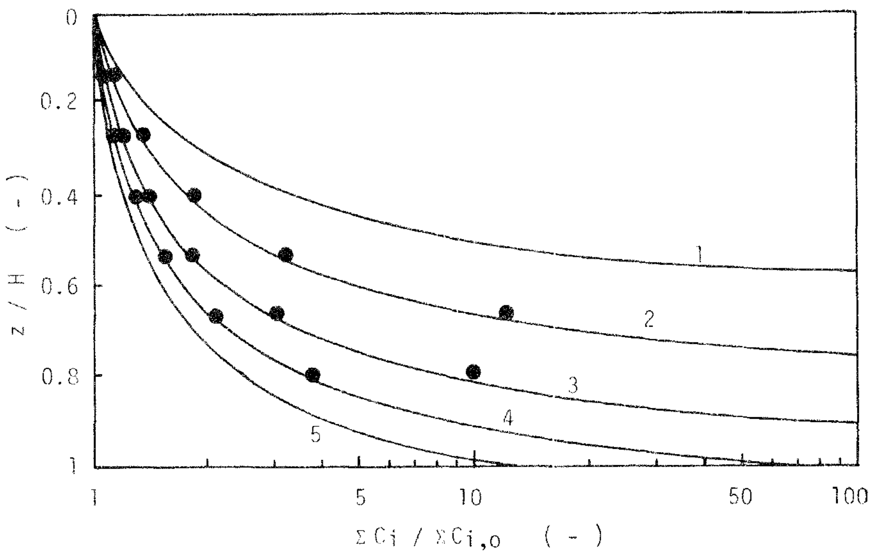

FIG. 13. Effect of the decay of turbulent energy supplied on the upper level of the suspension on the sedimentation behavior of monodispersed alumina particles ($d_p = 10$ μm): (1) $D_0 = 0.24 \times 10^{-4}$ m²/s, (2) $D_0 = 0.36 \times 10^{-4}$ m²/s, (3) $D_0 = 0.63 \times 10^{-4}$ m²/s, (4) $D_0 = 0.95 \times 10^{-4}$ m²/s, (5) $D_0 = 1.22 \times 10^{-4}$ m²/s. (Solid lines correspond to $\alpha_1 = 0.8$, $\alpha_2 = 3$, $\beta_1 = 0.8$, and $\beta_2 = 4.5$, while plots are experimental results.)

$D_{0,x}$, $D_{0,z}$	turbulent diffusion coefficient of a single solid particle (m²/s)
$D_{t,x}$, $D_{t,z}$	turbulent diffusion coefficient of solid particles (m²/s)
d_p	particle diameter (μm)
H	suspension height (m)
I	diffusion current (μA)
I'	fluctuating component of diffusion current (μA)
L	distance from the source of turbulence (m)
$R_E(\tau)$	Eulerian velocity correlation function (—)
t	time (s)
u	flow velocity (m/s)
$\bar{u}$	mean velocity (m/s)
u'	fluctuating velocity (m/s)
u'_m	fluctuating velocity observed (m/s)
u'_0	fluctuating velocity of continuous phase (m/s)
$v_{0,i}$	settling velocity of a single solid particle in ith class of size fraction (m/s)
$v_{s,i}$	settling velocity of solid particles in ith class of size fraction (m/s)
x, z	space coordinates

Greek

α_1, α_2	constants involved in Eq. (2)
β_1, β_2	constants involved in Eqs. (3) and (4)
ξ_1, ξ_2	constants involved in Eq. (16)
γ	constant involved in Eq. (8)
η	constant involved in Eq. (13)
Λ_f	integral space scale of turbulence (mm)
ν	kinematic viscosity (m^2/s)
T_E	Eulerian integral time scale (ms)
τ	time (ms)

REFERENCES

1. T. Neesse, *Freiberg. Forschungsh., A456,* 6 (1969).
2. T. Neesse, *Chem. Techn., 23,* 146 (1974).
3. H. Schubert and T. Neesse, in *Proceedings of the Tenth International Mineral Processing Congress* (M. J. Jones, ed.), Alden & Mowbray, Oxford, 1974, p. 213.
4. P. Koch, *Freiberg. Forschungsh., A546,* 5 (1975).
5. H. Schubert, *Neue Bergbautech., 7,* 446 (1977).
6. H. Schubert and C. Bischofberger, *Int. Miner. Process.,* 5, 131 (1978).
7. H. Schubert and C. Bischofberger, in *The 13th International Mineral Processing Congress, Warszawa, Vol. 2,* Warsaw, 1979, p. 353.
8. M. Nonaka, T. Inoue and T. Imaizumi, in *The 14th International Mineral Processing Congress, Vol. 3,* Toronto, 1982, p. 9.1.
9. W. E. Dobbins, *Trans. Am. Soc. Civ. Eng., 109,* 629 (1944).
10. T. Tatsumi, in *Ranryu,* Maki, Tokyo, 1964, 166 pp.
11. J. O. Hinze, in *Turbulence,* 2nd ed., McGraw-Hill, New York, 1975, 790 pp.
12. T. Mizushina, *Heat Transfer, 7,* 87 (1971).
13. S. Ito and S. Urushiyama, *Kagaku Kogaku, 32,* 267 (1968).
14. J. F. Richardson and W. N. Zaki, *Trans. Inst. Chem. Eng., 32,* 35 (1954).
15. K. J. Scott, *Trans. Inst. Min. Metall., 78,* C85 (1968).
16. S. Mirza and J. F. Richardson, *Chem. Eng. Sci., 34,* 447 (1979).
17. M. Nonaka, T. Inoue, and T. Imaizumi, *J. Min. Metall. Inst. Jpn., 93,* 371 (1977).
18. B. F. Towler and R. Y. K. Yang, *Chem. Eng. J., 12,* 81 (1976).

Received by editor November 1, 1983
Revised February 6, 1984